RSC Advances

PAPER

View Article Online
View Journal | View Issue

Cite this: *RSC Adv.*, 2020, **10**, 37675

Mucilage-capped silver nanoparticles for glucose electrochemical sensing and fuel cell applications†

Ziad Khalifa, *[a] Moustafa Zahran, [bc] Magdy A-H Zahran[b] and Magdi Abdel Azzem[b]

Received 27th August 2020
Accepted 30th September 2020

DOI: 10.1039/d0ra07359h

rsc.li/rsc-advances

A simple, cost-effective and green mucilage-capped silver nanoparticles (Mucilage-AgNPs) modified glassy carbon electrode (GC) composite was constructed for efficient and facile electrochemical oxidation of glucose for the first time. Mucilage-AgNPs were synthesized through the direct chemical reduction of Ag^+ by mucilage extracted from *Opuntia ficus-indica*. Mucilage-AgNPs were identified and characterized using ultraviolet-visible spectroscopy, transmission electron microscopy and square wave voltammetry. Modification of the GC with AgNPs was carried out *via* a transfer-sticking technique with an immobilization time of 1 h. The Mucilage-AgNPs/GC composite was studied as a possible anode for glucose oxidation in a biofuel cell. The composite resulted in glucose oxidation with a current density and power density of 85.7 μA cm^{-2} and 25.7 μW cm^{-2}, respectively. Glucose sensing using the Mucilage-AgNPs/GC composite was achieved successfully *via* two pathways: glucose oxidation and AgNP inhibition. The glucose oxidation-based sensor showed a lower detection limit of 0.01 mM and a linear range of 0.01 to 2.2 mM. The AgNPs inhibition-based sensor provides an indirect determination pathway of glucose with a detection limit of 0.1 mM and a linear range of 0.1 to 1.9 mM. AgNP inhibition is a novel pathway that could be used for determining a large number of organic and inorganic molecules. Overall, the Mucilage-AgNPs/GC is considered a pioneering composite for glucose sensing and fuel cell applications.

Introduction

Glucose is a vital molecule for humans due to its ability to provide the required energy for all types of physiological activities.[1] Recently, the electrochemical oxidation behavior of glucose has attracted considerable attention, not only for its determination in biological samples[2–4] but also as a sustainable fuel for fuel cells.[5,6] The glucose molecule can be oxidized theoretically to carbon and water, releasing 24 electrons. However, the oxidation process is much slower at the electrode surface, resulting in gluconic acid formation and the release of only two electrons.[7] The electrochemical oxidation of glucose at bare solid electrodes, such as platinum (Pt), gold (Au) and glassy carbon (GC) electrodes has been studied previously.[7] The glucose oxidation peak current is sensitive to the electrode surface area, thus increasing the electrode surface area through its modification with particular materials will optimize the glucose oxidation.[8] Metallic nanoparticles are known for their high surface area relative to their volume making them the appropriate choice for electrode modification.

Among the metallic nanoparticles, silver nanoparticles (AgNPs) show superior catalytic, electronic, optical, and electrochemical features making them the best choice for different medical, environmental and industrial applications.[9,10] Currently, AgNPs are fabricated efficiently through a number of chemical and physical techniques. However, most of these techniques are sophisticated, require high energy and result in negative environmental impacts.[11] Direct chemical reduction based on natural resources represents an attractive pathway that is simple, cheap, and green.[12,13] Recently, we reported the synthesis of AgNPs through direct chemical reduction using dissolved organic matter and natural latex to constructing pioneering electrochemical sensors for pesticides and dye determination in aqueous systems.[14,15]

AgNPs were used for glucose sensing *via* colorimetric techniques such as surface plasmon resonance (SPR), fluorescence and surface enhanced Raman spectroscopy.[16–18] Concerning the electrochemical techniques, AgNPs were used for glucose sensing and glucose fuel cell applications based on glucose oxidation.[19]

The catalytic oxidation of glucose optimization and efficient electrode modifier selection have directed researchers to examine various materials, such as carbon nanotubes,

[a]*Chemical Engineering Deparetment, Faculty of Engineering, The British University in Egypt, El Sherouk City, 11837, Egypt. E-mail: ziad.khalifa@bue.edu.eg*

[b]*Department of Chemistry, Faculty of Science, El-Menoufia University, Shibin El-Kom 32512, Egypt*

[c]*Menoufia Company for Water and Wastewater, Holding Company for Water and Wastewater, Menoufia 32514, Egypt*

† Electronic supplementary information (ESI) available: Tables S1 and S2: raw data associated with the calibration curves. Fig. S1: SWVs of 0–2.2 mM glucose oxidation at mucilage-AgNPs/GC (source files). See DOI: 10.1039/d0ra07359h

poly(allylamine hydrochloride), poly(styrenesulfonate), and chitosan, to enhance the catalytic efficacy of AgNPs.[8,20,21] Mucilage may be an excellent substance for the formation of Mucilage-AgNPs as electrode modifier for glucose oxidation owing to its ability to adsorb glucose efficiently.[22]

Mucilage is a pectic polysaccharide, which is enriched with galacturonic acid, galactose, arabinose, and xylose.[23] It was used for water clarification since ancient times. Recently, its role as a natural flocculant for arsenic removal has been reported.[24] Li *et al.* reported the excellent lubrication properties of mucilage that result from the hydration layer between the polymer nanosheets in mucilage.[25] Mucilage was used as food thickener, food emulsifier, and adhesive for lime and plasticizer.[26] Its capability to control diabetes has been studied.[22] In this study, we fabricated AgNPs using mucilage extracted from *Opuntia ficus-indica* as an efficient glassy carbon electrode (GC) modifier for glucose adsorption and subsequent oxidation. Mucilage-AgNPs/GC is a simple, sensitive, cost-effective and green composite for glucose oxidation for both sensing and fuel cell applications. Additionally, we report AgNPs inhibition sensor for glucose detection for the first time.

Experimental

Mucilage-AgNPs synthesis

Stems of *O. ficus* were collected from Shibin Al-Kom, Menoufia, Egypt and recognized by Professor ZakiTurki of Botany Department, Faculty of science, Menoufia University, Egypt. *O. ficus* stems were cut-off carefully for mucilage extraction. Aqueous mucilage extracts of different concentrations (10%, 20%, 40%, 60%, 80% and 100%) were prepared for Mucilage-AgNPs synthesis by heating a mixture of 20 mL of mucilage solution and 30 mL of 1 mM $AgNO_3$ (Cambrian Chemicals, 99.8% purity) aqueous solution at 55 °C. For Mucilage-AgNPs purification, the suspension was centrifuged at 6000 rpm for 30 min. The effect of mixing time and pH were studied for efficient stable AgNPs synthesis of the required size.

Mucilage-AgNPs characterization

Mucilage-AgNPs were identified and characterized using ultraviolet visible spectroscopy (UV-Vis), square wave voltammetry (SWV), particle size analyzer, and transmission electron microscopy (TEM). UV-Vis (UV-2450, Shimadzu, Japan) was used for SPR peak identification corresponding to AgNPs. SWV was studied using BAS Epsilon-EC (West Lafayette, IN 47906, USA) for identifying the potential value of Mucilage-AgNPs electrochemical oxidation which is important for nanoparticle size determination. For SWV analysis, a three-electrode setup based on GC (3 mm diameter) as the working electrode, platinum wire as the counter electrode and silver/silver chloride as the reference electrode was used. The particle size analyzer was used for size determination during optimization procedures, and TEM was used for size confirmation of AgNPs synthesized under optimized conditions.

Mucilage-AgNPs/GC composite preparation

First, GC was polished until obtaining a smooth and mirror surface using an alumina slurry before immersion in phosphate buffer solution (PBS) for electrolysis under 0.8 V for 40 min. Mucilage-AgNPs were deposited at the GC surface *via* the transfer-sticking technique.[14] The electrode was submerged in the nanoparticles stock suspension for 1 h for efficient adhesion.

Oxidation of glucose at mucilage-AgNPs/GC composite

SWV was used for studying the oxidation of glucose at Mucilage-AgNPs/GC composite in the potential range of −0.1 to 0.8 V. Additionally, oxidation of Mucilage-AgNPs at the GC electrode was studied for nanoparticles size detection as well as the Mucilage-AgNPs inhibition upon glucose addition. Both the oxidation of glucose and Mucilage-AgNPs was promoted with regard to immobilization time, scan rate, PBS pH, purification, and potential range. The SWVs of Mucilage-AgNPs/GC after addition of different glucose concentrations (0–1.9 mM) and (0–2.2 mM) were obtained for Mucilage-AgNPs inhibition and glucose oxidation sensors respectively. Straight lines that connect the minima before and after the Mucilage-AgNPs and glucose peak maximum were used for peak current determination. Calibration curves were analyzed using OriginPro 8.0 (Origin Lab Corporation, USA). The limit of detection (LOD) value was determined using eqn (1).

$$\mathrm{LOD} = 3\sigma/b \quad (1)$$

where (σ) is the standard deviation of the y-intercept and (b) is the slope of the calibration curve.[27] The slope value was used for sensitivity determination, where sensitivity = slope. The relative standard deviation (RSD) of the sensors was measured for six replicates. Ascorbic acid, urea, dopamine and uric acid were received from Sigma-Aldrich and employed for interferences study. Additionally, the suitability of the proposed sensors for glucose determination in human blood serum, which was obtained from a healthy subject as a real sample, was investigated. The results were compared to ones obtained from the biochemistry analyzer (Clinichem, Biomed Diagnostics) for authentication.

Results and discussion

Mucilage-AgNPs synthesis

Mucilage-AgNPs were synthesized by mixing silver nitrate solution with mucilage of *O. ficus via* direct chemical reduction. The efficacy of plant mucilage in the bioreduction and the subsequent capping is attributed to its reducing compounds.[23] Turning the colorless mucilage into a brownish suspension is regarded as a primary identification of Mucilage-AgNPs.[12,13] To obtain Mucilage-AgNPs with a controlled particle size, the mixing time, mucilage concentration and pH during heating at 55 °C were examined (Fig. 1). Controlling the particle size of Mucilage-AgNPs is essential for inhibition sensor construction and for increasing the surface area. Regarding the mixing time

effect, increasing the time from 5 min to 45 min resulted in a gradual AgNPs size reduction (Fig. 1A). Upon decreasing the metallic nanoparticles size, the suspension color turned from semi-dark to dark brown (Fig. 1A inset). This color change is attributed to the SPR of AgNPs, which mainly depends on the quantum size confinement. The mucilage concentration is also a significant factor for controlling the synthesis process. Sufficient mucilage material should be present for both silver ion (Ag^+) reduction and subsequent AgNPs capping. However, exceeding the mucilage content compared to Ag^+ in the suspension could make the synthesis process more difficult. Optimum synthesis was obtained by using a 60% mucilage concentration, as shown in Fig. 1B. However, pH plays a crucial role in stabilizing the AgNPs according to the chemistry of the capping layer. In our study, pH 8 was found to be suitable for preserving the AgNPs at a lower size without inducing any aggregation (Fig. 1C).

Mucilage-AgNPs characterization

Under the enhanced conditions of AgNPs synthesis, UV-Vis, SWV, and TEM were used for AgNPs identification and characterization. UV-Vis spectroscopy is an elegant tool for providing valuable information about metallic nanoparticles. It indicated the absorption peak (SPR peak) of AgNPs detected mainly at approximately 380 to 480 nm.[11] Our Mucilage-AgNPs showed SPR peak at 400 nm, confirming the nanoparticles synthesis (Fig. 2A). Additionally, this absorption wavelength corresponds to AgNPs of 15 to 20 nm.[28] Like UV-Vis, SWV could refer to the AgNPs size through the potential at which AgNPs electrochemically oxidized. Recently, we reported the role of the oxidation potential value in determining the AgNPs size.[15] The Mucilage-AgNPs had an electrochemical oxidation of approximately 0.01 V, which suggests an approximate size of 20 nm size approximately (Fig. 2B). TEM studies showed that AgNPs were in the size range of 10 to 20 nm, supporting UV-Vis and SWV results (Fig. 2C). This nanoparticles size is crucial not only for increasing the surface area of the electrode modifier but also for increasing the inhibition sensor efficiency.

The electrochemical properties of the bare and modified electrodes were studied by cyclic voltammetry (CV) in 5.0 mM potassium ferrocyanide ($K_4Fe(CN)_6 \cdot 3H_2O$) and 1.0 M KCl solution (Fig. 3). The GC electrode showed optimized oxidation and reduction peak currents when it was modified with Mucilage-AgNPs. Additionally, there was an observed reduction in the peak-to-peak separation (ΔE_p) value from 0.270 V to 0.185 V after modification representing a rapid electron transfer. The

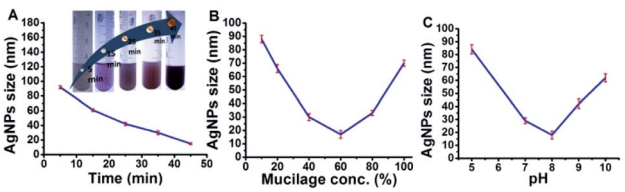

Fig. 1 Optimization of Mucilage-AgNPs size through mixing time (A), mucilage concentration (B) and pH (C).

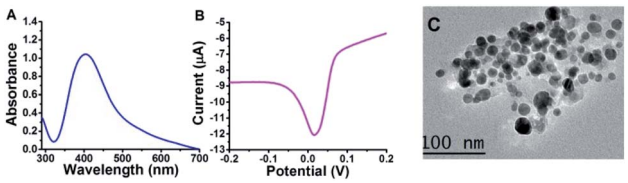

Fig. 2 Mucilage-AgNPs characterization using UV-Vis (A), SWV (B) and TEM (C).

optimization of redox peak currents and the reduction of ΔE_p value resulted from the electrocatalytic activity of AgNPs. The active surface areas of GC and Mucilage-AgNPs/GC were calculated according to the Randles–Sevcik equation (eqn (2)).

$$i_p = (2.69 \times 10^5) n^{3/2} A C D^{1/2} v^{1/2} \quad (2)$$

where i_p is the current (A), n is the number of transferred electrons in the redox reaction ($n = 1$), A is the electrode active surface area (cm^2), C is the concentration of $K_4Fe(CN)_6$ (mol cm^{-3}), D is the $K_4Fe(CN)_6$ diffusion coefficient (7.60×10^{-6} cm^2 s^{-1}), and v is the scan rate (V s^{-1}). The active surface areas of the GC and Mucilage-AgNPs/GC were 0.04 and 0.12 cm^2, respectively. The Mucilage-AgNPs/GC surface area was incremented three-fold in the presence of Mucilage-AgNPs at the GC electrode.

Glucose oxidation at mucilage-AgNPs/GC

The Mucilage-AgNPs/GC composite was successfully constructed by the transfer-sticking technique through direct immersion of the GC on the nanoparticles stock for 1 h for complete adsorption at the electrode surface before transferring it to the buffer solution for the electrochemical studies. Recently, we reported the transfer-sticking as the best technique for AgNPs immobilization compared to drop casting and sticking techniques.[14] The oxidation behaviors of both glucose and Mucilage-AgNPs at the electrode surface were studied (Fig. 4). There were two peaks detected at −0.3 and 0.01 V, corresponding to glucose and Mucilage-AgNPs oxidation peaks,

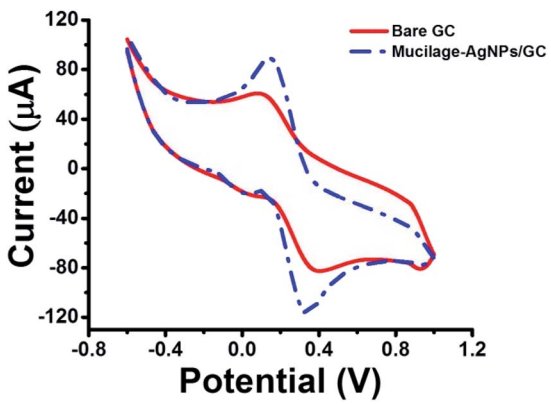

Fig. 3 Cyclic voltammogram of 5.0 mM $K_4Fe(CN)_6 \cdot 3H_2O$ in 1.0 M KCl at bare GC and Mucilage-AgNPs/GC electrodes, scan rate 0.05 V s^{-1}.

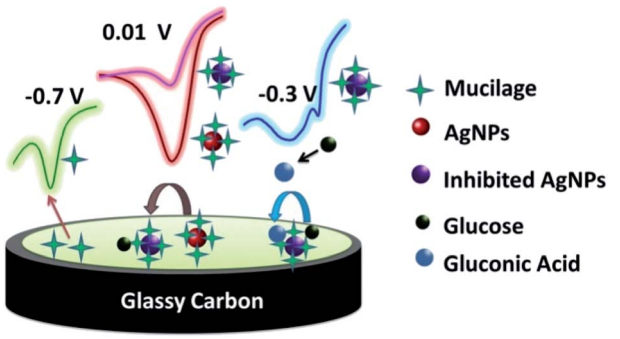

Fig. 4 Schematic representation of Mucilage-AgNPs oxidation at GC surface.

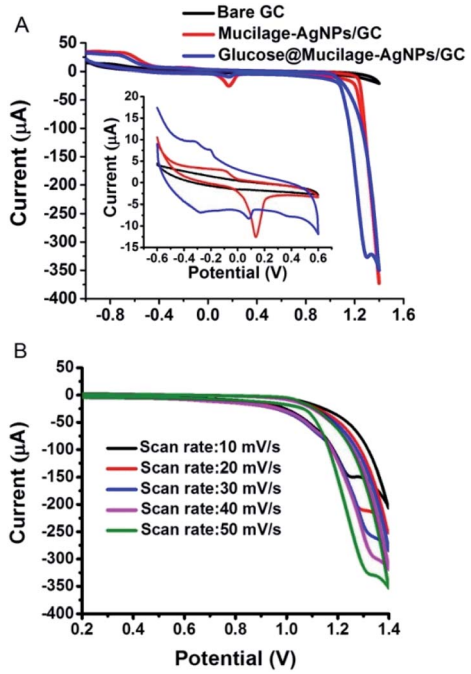

Fig. 5 Cyclic voltammogram of 1.0 mM glucose oxidation at Mucilage-AgNPs/GC in PBS pH 7.3 (A), and the effect of scan rate (B).

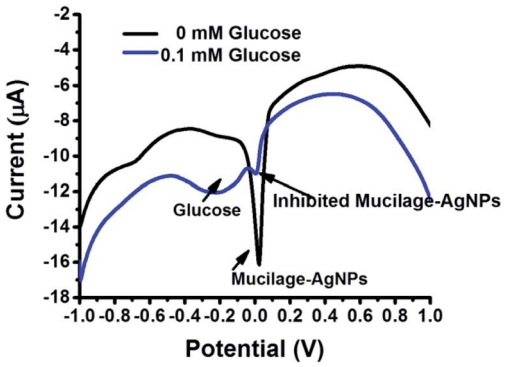

Fig. 6 SWV of 0.1 mM glucose at Mucilage-AgNPs/GC in PBS pH 7.3. SWV parameters: scan rate, 0.1 V s^{-1}; step potential, 0.004 V; frequency, 25 Hz; amplitude, 0.025.

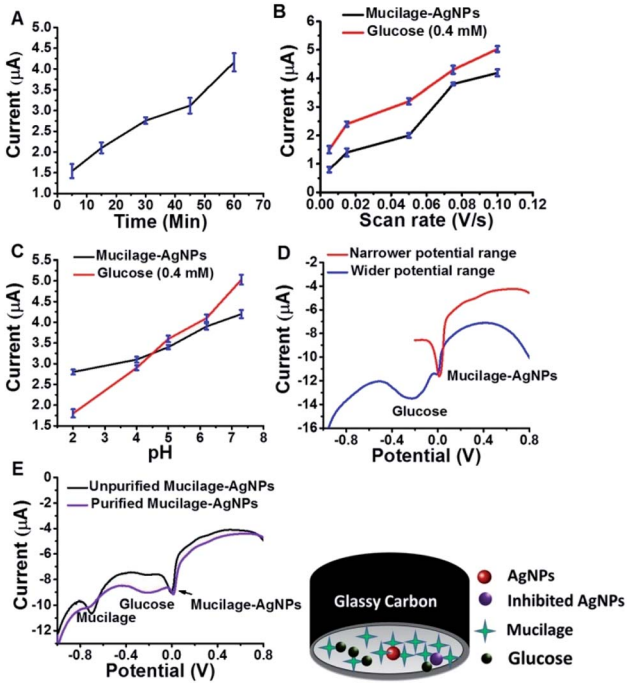

Fig. 7 Effect of immobilization time (A), scan rate (B), pH (C), potential range (D) and purification (E) on AgNPs and glucose oxidation.

respectively. The defined glucose oxidation peak (−0.3 V) was attributed to the oxidation of glucose to gluconic acid.[5] This directed us to study the applicability of Mucilage-AgNPs/GC in a glucose fuel cell as well as glucose sensing. However, we observed Mucilage-AgNPs peak current inhibition with glucose addition suggesting AgNPs as a novel inhibition sensor for glucose determination. The inhibition could be attributed to the effect of gluconic acid on the oxidation layer of the AgNPs.[29] In addition, a peak at −0.7 V suggested mucilage oxidation.

Table 1 Comparison of fuel cells performance

Anode material	Glucose (mM)	Current density (μA cm^{-2})	Power density (μW cm^{-2})	Ref.
Nafion/Pt	100	0.106	0.024	34
AgNPs/graphene oxide/GC	5	—	80	32
Au nanowire/GC	30	1340	126	35
Au-AgNPs/C	100	—	620	33
Mucilage-AgNPs/GC	1	85.7	25.7	This study

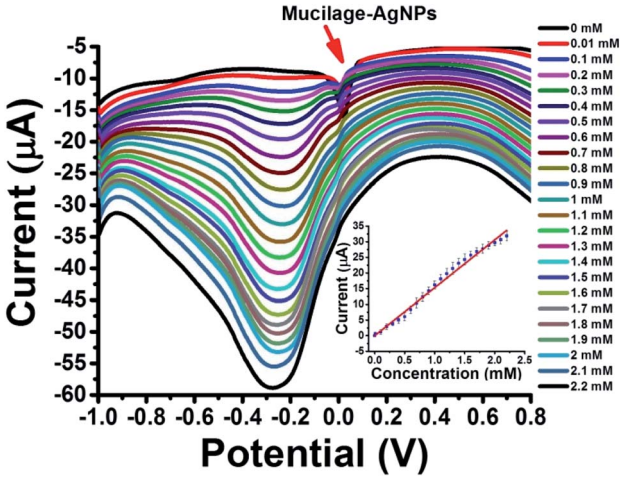

Fig. 8 SWV of glucose (0.01–2.2 mM) oxidation at Mucilage-AgNPs/GC in PBS pH 7.3 and the corresponding calibration curve.

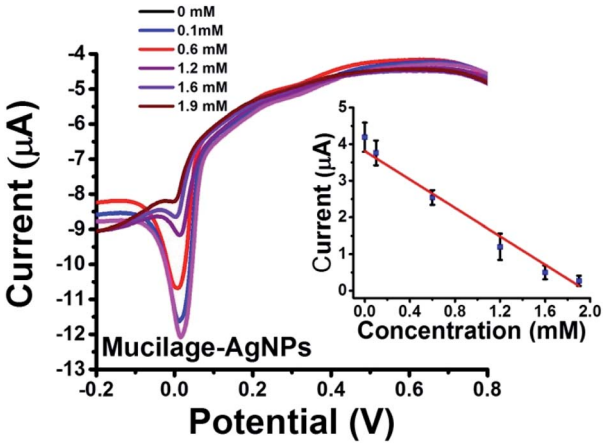

Fig. 9 SWV of Mucilage-AgNPs inhibition at GC and the corresponding calibration curve.

Table 2 Analytical parameters for glucose assessment

Sensor	Linear range (mM)	R^2	LOD (mM)	Sensi.	RSD (%)
Oxidation sensor	0.01–2.2	0.99	0.01	15	2.12
Inhibition sensor	0.1–1.9	0.98	0.1	1.9	2.26

Table 4 Interferences effect on glucose determination

	Signal change[a] (%)	
Interference	Direct glucose sensor	Inhibition sensor
Ascorbic acid	−3.8 ± 0.17	0.9 ± 0.11
Urea	−4.8 ± 0.16	1.3 ± 0.42
Dopamine	4.1 ± 0.11	1.2 ± 0.15
Uric acid	4.6 ± 0.13	0.8 ± 0.14

[a] 95% confidence interval calculated ($n = 6$).

Mucilage-AgNPs/GC-based glucose fuel cell

Replacing fossil fuels energy sources with cleaner and sustainable ones has become a pivotal issue. Glucose represents the most suitable fuel because of its availability, non-volatility, safety, and biocompatibility.[30] Glucose fuel cells are based on glucose oxidation for electricity generation. The glucose fuel cell could be microbial, enzymatic, or abiotic.[31] An abiotic one is preferred due to its simplicity, stability and toughness. In abiotic cell, glucose is oxidized directly in alkaline medium. This study reports a simple, sensitive, green, and cost effective glucose fuel cell using Mucilage-AgNPs/GC as the anode for glucose oxidation. Fig. 5A shows the cyclic voltammogram of glucose oxidation at the Mucilage-AgNPs/GC. In addition to the glucose oxidation to gluconic acid at −0.3 V, a peak appeared at approximately 1.3 V, where glucose was further oxidized under an oxygen evolution reaction. A linear dependence was detected for the anodic peak currents (1.3 V) and related scan rates at the Mucilage-AgNPs/GC in presence of 1.0 mM glucose in a PBS at pH 7.3, as shown in Fig. 5B. The fuel cell exhibited current density and power density of 85.7 μA cm^{-2} and 25.7 μW cm^{-2},

Table 3 Comparison between glucose electrochemical sensors[a]

Electrode material	Detection potential	Linear range (mM)	LOD (mM)	Ref.
Au nanowire/GC	0.3 V *vs.* SCE	Up to 12	0.02	35
PtRuNP-MWCNT/GC	−0.1 V *vs.* SCE	0.2–15	0.05	36
Cu/CuO/ZnO		0.1–1	0.18	37
RGO/CuNP/Au		0.01–1.2	0.0034	38
Au core/Ag shell nanorods/GC	−0.5 V *vs.* Pt	2 to 12	—	39
AgNPs $(PAH/PSS)_2$	0.6 V *vs.* SCE	0.02–23.3	0.02	21
AgNPs/PVA/Pt	−0.4 V *vs.* SCE	0.01–8	0.004	40
GOx/MnOxides/PE		0.56–5.55	0.29	41
Au/Ni/BDD		0.02–2	0.003	42
		2–9		
Mucilage-AgNPs/GC	−0.3 V *vs.* Ag/AgCl	0.01–2.2 (oxidation sensor)	0.01	This study
		0.1–1.9 (inhibition sensor)	0.1	

[a] SCE: saturated calomel electrode, MWCNT: multiwall carbon nanotube, RGO: reduced grapheme oxide, PAH: poly(allylamine hydrochloride), PAH: poly(styrenesulfonate), PVA: polyvinyl alcohol, PE: pencil graphite electrode, BDD: boron-doped diamond electrode.

Table 5 Glucose determination in human serum

Glucose concentration			Found glucose			Recovery	
Sample (mM)	Diluted sample (mM)	Added glucose (μM)	Analyzer	Oxi. ssensor	Inhibi. sensor	Glucose sensor	Inhibi. sensor
5.4	2.0	0	2.07	2.14	2.11	107	105.5
		100	2.13	2.19	2.18	104.3	103.8
		300	2.32	2.33	2.31	101.3	100.4
		500	2.51	2.47	2.52	98.8	100.8

respectively. The proposed anode resulted in a higher power density through oxidation of a lower concentration (1 mM) of glucose (Table 1). The role of AgNPs in optimizing the glucose fuel cell was studied previously. In an enzymatic-based fuel cell, reduced graphene oxide-AgNPs hybrid was used for enzyme adsorption to facilitate electron transfer between the enzyme and the electrode.[32] Additionally, the combination of the AgNPs with other metals such as gold (Au) and platinum (Pt), results in enhanced selectivity and power density performance. For example, Cuevas-Muñiz *et al.* reported the role of AgNPs in increasing the catalytic effect and power density of the Au/C electrode in glucose microfluidic fuel cell.[33] In our study, mucilage interacted with AgNPs resulted in efficient glucose adsorption at the modified electrode facilitating the oxidation process with a high power energy performance. The interaction of glucose with mucilage for controlling the glucose level in blood serum was studied previously.[22]

Optimized conditions for glucose sensing using mucilage-AgNPs/GC

SWV was used to study the efficacy of the modified electrode for glucose determination in the potential range of −1.0 to 0.8 V (Fig. 6). For efficient glucose and AgNPs oxidation, different parameters, such as immobilization time, scan rate, pH, purification, and potential range were studied. The optimized immobilization time, scan rate, and pH were 1 h, 0.1 V s^{-1} and 7.3, respectively (Fig. 7 A–C). The effect of potential range is important for optimizing the inhibition sensor. Obviously, the oxidation current of AgNPs was optimized when the starting potential increased to −0.1 V (Fig. 7D). Thus, the Mucilage-AgNPs interacted with glucose, leading to AgNPs inhibition without oxidation of glucose to gluconic acid. Additionally, gluconic acid could interact with Mucilage-AgNPs causing inhibition as well. The effect of gluconic acid on oxidation layer inhibition of the AgNPs in suspension was previously studied.[29] Purification of the Mucilage-AgNPs from excess mucilage before electrode modification is critical for oxidation of both glucose and AgNPs. In the case of Mucilage-AgNPs unpurification, the excess mucilage in suspension will adsorb at the electrode surface, leading to less adsorption and thus reduced AgNPs oxidation current. However, the adsorbed mucilage could bind with some glucose molecules, hindering its interaction as Mucilage-AgNPs (Fig. 7E).

Mucilage-AgNPs/GC for glucose sensing based on glucose oxidation

Mucilage-AgNPs/GC was studied as a simple, sensitive, cost effective, and green sensor for glucose assessment. The glucose detection is based on two pathways: glucose oxidation to gluconic acid with a peak detected at −0.3 V (direct pathway) and AgNPs inhibition *via* glucose with a peak around 0.01 V (indirect pathway). Regarding the direct pathway, different concentrations of glucose (0–2.2 mM) in PBS at pH 7.3 were oxidized at the electrode composite using SWV under optimized conditions. Fig. 8 shows the SWV of glucose oxidation at Mucilage-AgNPs/GC and the corresponding calibration curve. Obviously, AgNPs oxidation peak gradually disappeared owing to AgNPs electrochemical inhibition through its interaction with additional glucose. However, Mucilage-AgNPs inhibition didn't affect the glucose oxidation at the Mucilage-AgNPs/GC composite, as shown in Fig. 8. The LOD and RSD of the sensor were 0.05 and 2.12, respectively confirming its suitability for glucose assessment (Table 2). Some of the reported electrochemical glucose sensors are listed in Table 3.

Mucilage-AgNPs/GC for glucose sensing based on AgNPs inhibition

To our knowledge, using AgNPs inhibition as sensor was not previously studied. In the present investigation, we report AgNPs inhibition as a novel sensor for glucose assessment. Mucilage-AgNPs were inhibited gradually by increasing the glucose concentration under optimized conditions (Fig. 9). The sensor showed LOD and RSD of 0.1 and 2.26, respectively. The AgNPs oxidation behavior at the electrode surface is of great interest. Recently, we reported novel electrochemical sensors based on aggregation and replacement of AgNPs at GC by organic pollutants. AgNPs inhibition represents another pioneering phenomenon for determination of many organic and inorganic compounds.

Interference study

The selectivity of the two sensors was investigated by studying ascorbic acid, urea, dopamine, and uric acid interferences. The voltammetric responses of 1 mM glucose in presence of 0.1 mM of each interference were determined. Significantly, the signal change which did not exceed 5%, was accepted. Glucose showed an acceptable change (<5%) in the presence of the interferences

under investigation (Table 4). The inhibition sensor showed brilliant selectivity with slight signal change compared to the direct glucose sensor. AgNPs inhibition pathway is preferred over the direct oxidation in case of high concentrations of interferences. Therefore, the selection of the suitable pathway depends on the conditions of sample containing the analyte.

Real samples

Glucose was determined in a human blood sample using direct glucose and inhibition sensors. The human blood sample was diluted to 2 mM before spiking with the glucose concentrations. The responses of both sensors to glucose in spiked samples were determined and compared to a biochemistry analyzer for authentication. Both sensors showed high selectivity towards glucose with accepted recovery values (Table 5).

Conclusions

A facile synthesis process for Mucilage-AgNPs/GC composite was developed for glucose oxidation. After glucose addition to PBS at pH 7.3, the mucilage capping layer of AgNPs interacted with it efficiently, making the oxidation process easier and efficient. To optimize the oxidation process, different parameters, such as immobilization time, scan rate, pH, purification, and potential range were studied. Under optimized conditions, the suitability of Mucilage-AgNPs/GC as an anode in a biofuel cell was approved. Additionally, Mucilage-AgNPs/GC composite was studied as dual sensor for glucose through direct glucose oxidation and AgNPs inhibition. Mucilage-AgNPs/GC represents a simple, green and cost-effective composite for glucose sensing and glucose-based fuel cell applications.

Ethical statement

All human blood sampling and experiments were performed in accordance with the relevant Egyptian laws and guidelines and approved by the ethics committee at Menoufia University. Informed consents were obtained from human participants of this study.

Conflicts of interest

There are no conflicts to declare.

Acknowledgements

The authors acknowledge the scientific donation of Alexander von Humboldt Foundation.

Notes and references

1 K. Justice Babu, S. Sheet, Y. S. Lee and G. Gnana Kumar, Three-dimensional dendrite Cu–Co/reduced graphene oxide architectures on a disposable pencil graphite electrode as an electrochemical sensor for nonenzymatic glucose detection, *ACS Sustainable Chem. Eng.*, 2018, **6**, 1909–1918.

2 K. Hassan, G. Elhaddad and M. A. Azzem, Simultaneous determination of ascorbic acid, uric acid and glucose using glassy carbon electrode modified by nickel nanoparticles at poly 1, 8-diaminonaphthalene in basic medium, *J. Electroanal. Chem.*, 2014, **728**, 123–129.

3 K. M. Hassan and M. A. Azzem, Electrocatalytic oxidation of ascorbic acid, uric acid, and glucose at nickel nanoparticles/poly (1-amino-2-methyl-9, 10-anthraquinone) modified electrode in basic medium, *J. Appl. Electrochem.*, 2015, **45**, 567–575.

4 A. Hathoot, U. Yousef, A. Shatla and M. Abdel-Azzem, Voltammetric simultaneous determination of glucose, ascorbic acid and dopamine on glassy carbon electrode modified byNiNPs@ poly 1, 5-diaminonaphthalene, *Electrochimicaacta*, 2012, **85**, 531–537.

5 M. de Sá and L. Brandão, Non-enzymatic direct glucose fuel cells (DGFC): a novel principle towards autonomous electrochemical biosensors, *Int. J. Hydrogen Energy*, 2019, in press.

6 K. Hassan, Z. Khalifa, G. Elhaddad and M. A. Azzem, The role of electrolytically deposited palladium and platinum metal nanoparticles dispersed onto poly (1, 8-diaminonaphthalene) for enhanced glucose electrooxidation in biofuel cells, *Electrochim. Acta*, 2020, 136781.

7 A. Brouzgou and P. Tsiakaras, Electrocatalysts for glucose electrooxidation reaction: a review, *Top. Catal.*, 2015, **58**, 1311–1327.

8 Y. Liu, *et al.*, An antibacterial nonenzymatic glucose sensor composed of carbon nanotubes decorated with silver nanoparticles, *Electroanalysis*, 2015, **27**, 1138–1143.

9 M. Zahran and A. H. Marei, Innovative natural polymer metal nanocomposites and their antimicrobial activity, *Int. J. Biol. Macromol.*, 2019, **136**, 586–596.

10 K. M. Hassan, G. M. Elhaddad and M. AbdelAzzem, Voltammetric determination of cadmium (II), lead (II) and copper (II) with a glassy carbon electrode modified with silver nanoparticles deposited on poly (1, 8-diaminonaphthalene), *Microchim. Acta*, 2019, **186**, 440.

11 M. Zahran, M. El-Kemary, S. Khalifa and H. El-Seedi, Spectral studies of silver nanoparticles biosynthesized by Origanummajorana, *Green Process. Synth.*, 2018, **7**, 100–105.

12 E. I. El-Aswar, M. M. Zahran and M. El-Kemary, Optical and electrochemical studies of silver nanoparticles biosynthesized by Haplophyllumtuberculatum extract and their antibacterial activity in wastewater treatment, *Mater. Res. Express*, 2019, **6**, 105016.

13 M. El-Kemary, M. Zahran, S. A. Khalifa and H. R. El-Seedi, Spectral characterisation of the silver nanoparticles biosynthesised using Ambrosia maritima plant, *Micro & Nano Lett.*, 2016, **11**, 311–314.

14 M. Zahran, Z. Khalifa, M. A.-H. Zahran and M. Abdel Azzem, Dissolved Organic Matter-Capped Silver Nanoparticles for Electrochemical Aggregation Sensing of Atrazine in Aqueous Systems, *ACS Appl. Nano Mater.*, 2020, **3**, 3868–3875.

15 M. Zahran, Z. Khalifa, M. A.-H. Zahran and M. A. Azzem, *Natural Latex-Capped Silver Nanoparticles for Two-way Electrochemical Displacement Sensing of Eriochrome Black T*. ElectrochimicaActa, 2020, p. 136825.
16 X. Sun, S. Stagon, H. Huang, J. Chen and Y. Lei, Functionalized aligned silver nanorod arrays for glucose sensing through surface enhanced Raman scattering, *RSC Adv.*, 2014, **4**, 23382–23388.
17 J. Tashkhourian, M. Akhond, S. Hooshmand and M. Afsharinejad, A nanosensor for determination of glucose based on silver nanoparticles as fluorescence probes, *J. Iran. Chem. Soc.*, 2015, **12**, 2023–2030.
18 J. Tashkhourian, M. Hormozi-Nezhad, J. Khodaveisi and R. Dashti, A novel photometric glucose biosensor based on decolorizing of silver nanoparticles, *Sens. Actuators, B*, 2011, **158**, 185–189.
19 H. Quan, S.-U. Park and J. Park, Electrochemical oxidation of glucose on silver nanoparticle-modified composite electrodes, *Electrochim. Acta*, 2010, **55**, 2232–2237.
20 J. Lin, C. He, Y. Zhao and S. Zhang, One-step synthesis of silver nanoparticles/carbon nanotubes/chitosan film and its application in glucose biosensor, *Sens. Actuators, B*, 2009, **137**, 768–773.
21 P. Viswanathan, Y. J. Kim and J. D. Hong, Nanoporous silver submicrocubes layer by layer encapsulated with polyelectrolyte films: nonenzymatic catalysis for glucose monitoring, *Langmuir*, 2020, **36**, 3452–3460.
22 M. Sangeethapriya and P. Siddhuraju, Health related functional characteristics and antioxidant potential of mucilage (dietary fiber) from Zizyphusmauritiana fruits, *Food Sci. Hum. Well.*, 2014, **3**, 79–88.
23 D. I. Fox, T. Pichler, D. H. Yeh and N. A. Alcantar, Removing heavy metals in water: the interaction of cactus mucilage and arsenate (As (V)), *Environ. Sci. Technol.*, 2012, **46**, 4553–4559.
24 D. I. Fox, D. M. Stebbins and N. A. Alcantar, Combining ferric salt and cactus mucilage for arsenic removal from water, *Environ. Sci. Technol.*, 2016, **50**, 2507–2513.
25 J. Li, Y. Liu, J. Luo, P. Liu and C. Zhang, Excellent lubricating behavior of Braseniaschreberi mucilage, *Langmuir*, 2012, **28**, 7797–7802.
26 F. León-Martínez, J. Rodriguez-Ramirez, L. Medina-Torres, L. M. Lagunas and M. Bernad-Bernad, Effects of drying conditions on the rheological properties of reconstituted mucilage solutions (Opuntiaficus-indica), *Carbohydr. Polym.*, 2011, **84**, 439–445.
27 A. Shrivastava and V. B. Gupta, Methods for the determination of limit of detection and limit of quantitation of the analytical methods, *Chron. Young Sci.*, 2011, **2**, 21.
28 L. Mulfinger, *et al.*, Synthesis and study of silver nanoparticles, *J Chem. Educ.*, 2007, **84**, 322.
29 R. Janardhanan, M. Karuppaiah, N. Hebalkar and T. N. Rao, Synthesis and surface chemistry of nano silver particles, *Polyhedron*, 2009, **28**, 2522–2530.
30 K. Torigoe, *et al.*, High-Power Abiotic Direct Glucose Fuel Cell Using a Gold–Platinum Bimetallic Anode Catalyst, *ACS Omega*, 2018, **3**, 18323–18333.
31 M. Irfan, *et al.*, High-performance glucose fuel cell with bimetallic Ni–Co composite anchored on reduced graphene oxide as anode catalyst, *Renewable Energy*, 2020, **155**, 1118–1126.
32 F. Qu, X. Ma, Y. Hui, F. Chen and Y. Gao, Preparation of Close-Packed Silver Nanoparticles on Graphene to Improve the Enzyme Immobilization and Electron Transfer at Electrode in Glucose/O2 Biofuel Cell, *Chin. J. Chem.*, 2017, **35**, 1098–1108.
33 F. Cuevas-Muñiz, *et al.*, Glucose microfluidic fuel cell based on silver bimetallic selective catalysts for on-chip applications, *J. Power Sources*, 2012, **216**, 297–303.
34 S. Xu and S. D. Minteer, Enzymatic biofuel cell for oxidation of glucose to CO2, *ACS Catal.*, 2012, **2**, 91–94.
35 L. Yang, *et al.*, Facile fabrication of network film electrodes with ultrathin Au nanowires for nonenzymatic glucose sensing and glucose/O2 fuel cell, *Biosens. Bioelectron.*, 2014, **52**, 105–110.
36 F. Xiao, F. Zhao, D. Mei, Z. Mo and B. Zeng, Nonenzymatic glucose sensor based on ultrasonic-electrodeposition of bimetallic PtM (M= Ru, Pd and Au) nanoparticles on carbon nanotubes–ionic liquid composite film, *Biosens. Bioelectron.*, 2009, **24**, 3481–3486.
37 S. SoYoon, A. Ramadoss, B. Saravanakumar and S. J. Kim, Novel Cu/CuO/ZnO hybrid hierarchical nanostructures for non-enzymatic glucose sensor application, *J. Electroanal. Chem.*, 2014, **717**, 90–95.
38 Q. Wang, Q. Wang, M. Li, S. Szunerits and R. Boukherroub, Preparation of reduced graphene oxide/Cu nanoparticle composites through electrophoretic deposition: application for nonenzymatic glucose sensing, *RSC Adv.*, 2015, **5**, 15861–15869.
39 X. Yang, Y. Wang, Y. Liu and X. Jiang, A sensitive hydrogen peroxide and glucose biosensor based on gold/silver core–shell nanorods, *Electrochim. Acta*, 2013, **108**, 39–44.
40 M. R. Guascito, D. Chirizzi, R. A. Picca, E. Mazzotta and C. Malitesta, Ag nanoparticles capped by a nontoxic polymer: Electrochemical and spectroscopic characterization of a novel nanomaterial for glucose detection, *Mater. Sci. Eng. C*, 2011, **31**, 606–611.
41 P. Prasertying, *et al.*, Modified pencil graphite electrode as a low-cost glucose sensor, *Journal of Science: Advanced Materials and Devices*, 2020, **5**, 330–336.
42 K. Yao, *et al.*, Fabrication of Au/Ni/boron-doped diamond electrodes *via* hydrogen plasma etching graphite and amorphous boron for efficient non-enzymatic sensing of glucose, *J. Electroanal. Chem.*, 2020, 114264.

